Applied Catalysis B: Environmental 100 (2010) 282–288

Contents lists available at ScienceDirect

Applied Catalysis B: Environmental

journal homepage: www.elsevier.com/locate/apcatb

Catalytic wet air oxidation of formic acid over Pt/$Ce_xZr_{1-x}O_2$ catalysts at low temperature and atmospheric pressure

Shaoxia Yang[a,b], Michèle Besson[a], Claude Descorme[a,*]

[a] Institut de recherches sur la catalyse et l'environnement de Lyon (IRCELYON), UMR 5256 CNRS/University of Lyon, 2 Avenue Albert Einstein, 69626 Villeurbanne Cedex, France
[b] National Engineering Laboratory for Biomass Power Generation Equipment, School of Renewable Energy, North China Electric Power University, Beijing, 102206, China

ARTICLE INFO

Article history:
Received 26 April 2010
Received in revised form 29 July 2010
Accepted 5 August 2010
Available online 12 August 2010

Keywords:
Catalytic wet air oxidation
Formic acid
$Ce_xZr_{1-x}O_2$
Platinum
Oxygen mobility

ABSTRACT

$Ce_xZr_{1-x}O_2$-based Pt catalysts were investigated in the catalytic wet air oxidation (CWAO) of formic acid at low temperature (294–326 K) under atmospheric pressure in order to evaluate the impact of the high oxygen mobility over the ceria–zirconia supports on the catalytic performances. The effect of the support composition, the Pt loading and the reaction conditions (reaction temperature, formic acid concentration, oxygen partial pressure) was studied. The bare supports, in the absence of any active metal, appeared to be only slightly active. The 0.080 wt.%Pt/$Ce_{0.9}Zr_{0.1}O_2$ catalyst (0.5 g L^{-1}) exhibited the best performances: 100% formic acid (5 g L^{-1}) conversion was achieved after 360 min at 326 K under atmospheric pressure. The reaction apparent activation energy was ca. 36 ± 4 kJ mol^{-1}. In the lowest temperature range ($T \leq 313$ K), the initial reaction rate was proportional to the dissolved oxygen concentration and, accordingly, the reaction order with respect to oxygen was ca. 1 ± 0.1. The oxygen transfer to the active site was rate limiting and formic acid saturated the catalyst surface. More interestingly, from ca. 326 K, the reaction order with respect to formic acid increased to ca. 0.5 ± 0.1 and the reaction order with respect to oxygen decreased to 0.8 ± 0.1, indicating that oxygen might already be efficiently activated on the $Ce_xZr_{1-x}O_2$ mixed oxide supports even under moderate temperature conditions.

1. Introduction

Industrial wastewaters produced by chemical, petrochemical, pharmaceutical, textile and agricultural plants frequently contain highly concentrated, toxic and hazardous organic compounds. New technologies are tentatively developed for treating such effluents. Indeed, the application of biological technologies, the most common and widespread methods to treat wastewaters, is limited whenever bio-toxic compounds are present. Furthermore, incineration is certainly an effective process to oxidize highly concentrated organic compounds (chemical oxygen demand >100 g L^{-1}); however, detrimental dioxins and fly ashes are inevitably produced and potentially transferred to the atmosphere. Other technologies, such as the electrochemical oxidation, the Fenton process, the photocatalytic oxidation or the ozonation have been developed. Unfortunately, these technologies were shown to be really efficient only at low concentration in organic pollutants [1,2].

Wet air oxidation (WAO) has been proven as an effective technology to treat hazardous, toxic and highly concentrated industrial wastewaters, ultimately into CO_2, H_2O and other innocuous end products at high temperature (398–593 K) and pressure (0.5–20 MPa), using oxygen as the oxidant [3,4]. Using a catalyst, the operating conditions could be significantly lowered, the oxidation rate was increased and the reaction time could be shortened [5–9]. Heterogeneous catalysts appeared as the most promising ones since the separation of the dissolved metal ions from the effluents at the end of the reaction is not necessary anymore. Among heterogeneous catalysts, noble metal (Ru, Pt, Pd, Ag, Ir, etc.) supported catalysts were already applied to treat a large range of pollutants (olive oil mill effluents, coke-plant wastewaters, dyes, phenol, ammonia, toxic nitrogen containing compounds, carboxylic acids, etc.) and exhibited high performances and stabilities [10–15]. Carbon materials [16–19], transition metal oxides [20–22] and CeO_2-based catalysts [23,24] were also implemented in the CWAO of organic compounds and exhibited good performances.

Low molecular weight carboxylic acids gained some attention since they often appear as refractory intermediates in the oxidation of complex organic compounds. Moreover, these acids are valuable reagents, which are commonly used in the production of commercial organic products and which, in turn, frequently appear in the corresponding industrial wastewaters. Some studies showed that some of these acids, including glyoxalic, oxalic, propionic, acetic and formic acids, are readily oxidized into CO_2 and H_2O at high temperature and pressure in the absence of any catalyst [25,26]. Noble metal-based (Pt, Ir and Ru) catalysts, supported on carbon materials, TiO_2 or Al_2O_3 have also been used to treat carboxylic acids

* Corresponding author. Tel.: +33 4 7244 5307; fax: +33 4 7244 5399.
E-mail address: claude.descorme@ircelyon.univ-lyon1.fr (C. Descorme).

0926-3373/$ – see front matter © 2010 Elsevier B.V. All rights reserved.
doi:10.1016/j.apcatb.2010.08.004

and exhibited good performances. Pt/Al_2O_3, Pt/C and Ru/graphite catalysts were shown to be active in the CWAO of formic and acetic acids [27–31]. The stability of the support under the applied reaction conditions (high temperature, low pH) is an important issue. In the past decades, CeO_2 and CeO_2-based mixed oxides have been paid a lot of attention since they are active and stable under the CWAO operating conditions. Furthermore, such oxides exhibited enhanced oxygen activation properties which were shown to be beneficial for a number of reactions, such as three-way catalysis, methane reforming, water-gas shift and CWAO [32–36].

In this paper, Pt catalysts supported on $Ce_xZr_{1-x}O_2$ mixed oxides were synthesized and evaluated in the CWAO of formic acid under atmospheric pressure at moderate reaction temperature. The effect of the support composition, the Pt loading and the operating conditions (reaction temperature, formic acid concentration, oxygen partial pressure) on the catalytic performances was investigated. Some preliminary kinetic studies were also performed to get a better insight in the reaction mechanism. The main objective of this study was indeed to determine how the $Ce_xZr_{1-x}O_2$ mixed oxide supports might help to the oxygen transfer up to the active sites, even under moderate reaction conditions and impact on the catalyst performances.

2. Experimental

2.1. Catalysts preparation

The $Ce_xZr_{1-x}O_2$ oxides, with x varying from 0 (ZrO_2) to 1 (CeO_2), were prepared by (co)-precipitation. An aqueous solution of 0.9 mol L^{-1} $Ce(NO_3)_3$ and/or 0.1 mol L^{-1} $ZrOCl_2$ was added dropwise in a 0.5 mol L^{-1} ammonia solution under continuous and vigorous stirring. Precipitation occurred almost instantaneously and ammonia was further added to the solution to reach an alkaline pH of 10. The mixture was further aged at 358 K for 8 h while the pH was maintained at ca. 10. Afterwards, the precipitate was (i) sequentially washed with distilled water and ethanol to remove the chlorine ions and (ii) finally dried at 393 K overnight. The received solid was grinded and subsequently calcined at 773 K for 6 h under flowing air (60 L h^{-1}) in order to receive the $Ce_xZr_{1-x}O_2$ mixed oxides.

The Pt catalysts were prepared via wet impregnation using the $Pt(NH_3)_4(NO_3)_2$ salt as the metal precursor. The $Ce_xZr_{1-x}O_2$ support was added to the aqueous Pt solution. The mixture was stirred for 2 h at room temperature and then evaporated at 323 K under reduced pressure (ca. 50 mbar) for 3 h to remove the water. The solid was finally reduced under flowing H_2 (60 L h^{-1}) at 483 K for 2 h [37].

2.2. Catalysts characterization

X-ray diffraction (XRD) patterns (20–80°) were obtained on a Siemens D5005 diffractometer, using the Cu Kα radiation (λ = 0.15406 nm) to investigate the crystal structure of the $Ce_xZr_{1-x}O_2$ mixed oxides. The average crystallite size of the mixed oxides (D) was estimated using the Debye–Scherrer equation and the crystal composition was extracted from the diffractograms, assuming the oxides to be solid solutions and using the Vegard's law [38].

The specific surface area of the mixed oxides was determined by nitrogen adsorption at 77 K using a Micromeritics ASAP 2020 apparatus. Before the analysis, the sample was evacuated at 573 K for 3 h.

The pH at the point of zero charge (pH_{PZC}) of the mixed oxides was measured according to the method developed by Moriwaki et al. [39].

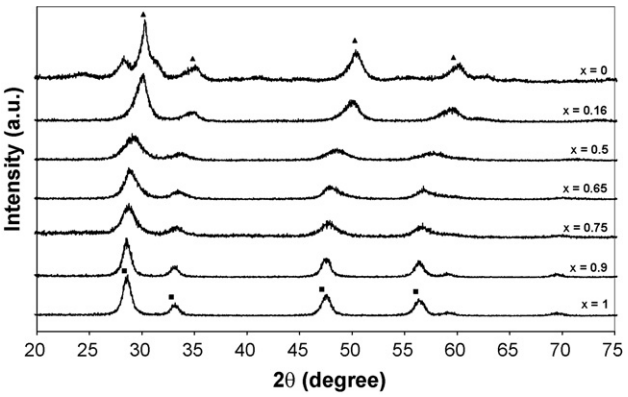

Fig. 1. XRD patterns of $Ce_xZr_{1-x}O_2$ supports (x = 1, 0.9, 0.75, 0.65, 0.5, 0.16 or 0) [■, ▲: main CeO_2 and ZrO_2 diffraction lines, respectively].

2.3. Catalytic wet air oxidation (CWAO) studies

CWAO experiments were carried out at atmospheric pressure in a semi-batch glass reactor. The reactor was thermostated using an oil bath and equipped with a thermocouple (measurement and regulation), a continuous air/O_2 inlet, through a sparger, directly into the reaction mixture, a sampling tube and a condenser open to the atmosphere to prevent any evaporation of the reaction mixture. At the beginning, 300 mL of a 5 g L^{-1} formic acid solution (TOC_0 ca. 1305 mg_C L^{-1}) and a fixed amount of catalyst were loaded into the reactor. Then, N_2 was bubbled into the reactor under vigorous stirring to remove any trace of oxygen. Finally, the reactor was heated up to the desirable temperature and, when the temperature was stabilized, air or O_2 was introduced in the reactor. This point was defined as "zero" time. During the reaction, the oxidant flow was fixed at 0.45 L min^{-1}. The dissolved O_2 concentration in the solution was measured using a Dissolved Oxygen Pocket Meter Oxi 315i, which could only be operated up to 323 K maximum. In all cases, the measured oxygen concentration was in perfect agreement with the expected values (ca. 8.9, 7.4, 6.4 and 5.2 mg L^{-1} at 294, 304, 313 and 326 K, respectively) and no barrier whatsoever to the oxygen dissolution in the aqueous phase was evidenced.

Samples were periodically withdrawn from the reactor and further analyzed via HPLC to follow the evolution of the formic acid concentration. The HPLC system was equipped with a CarboSep Coregel-87H3 column and a UV-detector set at 210 nm. The mobile phase was an aqueous sulphuric acid solution (0.005 M) and the flow rate was fixed at 0.5 mL min^{-1}.

The final solution was further analyzed by ICP-AES to check for any possible Pt, Ce or Zr leaching.

Noteworthy, most experiments were repeated two to three times, in particular to ascertain the reproducibility of the different experiments. Average reaction rates were reported whenever applicable. Differences not larger than ±5% were observed.

3. Results and discussion

3.1. Characterization of the supports

Fig. 1 shows the diffraction patterns of the $Ce_xZr_{1-x}O_2$ supports and Table 1 summarizes the main characteristics of the mixed oxides (lattice parameter, crystallite size) derived from these diffractograms.

For Ce ≥0.5 at.%, the main diffraction lines of the $Ce_xZr_{1-x}O_2$ mixed oxides are observed at ca. 2θ = 28.6°, 33.1°, 47.5° and 56.4°. These lines are characteristic of the fluorite-type structure. No additional peak characteristic of the ZrO_2 tetragonal phase is observed. Conclusively, it might be assumed that these supports exist as

Table 1
Structural and textural characteristics of the $Ce_xZr_{1-x}O_2$ mixed oxides.

Support	BET ($m^2\,g^{-1}$)	a[a] (nm)	D[b] (nm)	Crystal composition (XRD)	Chemical composition (ICP-OES)	pH_{PZC}
CeO_2	101	5.4112	8.7	CeO_2	CeO_2	7.0
$Ce_{0.9}Zr_{0.1}O_2$	102	5.4112	8.6	CeO_2	$Ce_{0.9}Zr_{0.1}O_2$	7.4
$Ce_{0.75}Zr_{0.25}O_2$	148	5.3490	5.1	$Ce_{0.76}Zr_{0.24}O_2$	$Ce_{0.75}Zr_{0.25}O_2$	6.5
$Ce_{0.65}Zr_{0.35}O_2$	131	5.3775	5.5	$Ce_{0.87}Zr_{0.13}O_2$	$Ce_{0.65}Zr_{0.35}O_2$	7.0
$Ce_{0.5}Zr_{0.5}O_2$	151	5.3049	4.4	$Ce_{0.60}Zr_{0.40}O_2$	$Ce_{0.5}Zr_{0.5}O_2$	6.0
$Ce_{0.16}Zr_{0.84}O_2$	152	3.6149	5.3	–	$Ce_{0.16}Zr_{0.84}O_2$	5.4
ZrO_2	137	3.5984	5.7	–	ZrO_2	5.5

[a] a, lattice parameter.
[b] D, oxide crystallite size.

mixed oxides. It is also found that: (1) the diffraction lines get broader as the Zr content increases, indicating that the crystallite size decreases, as shown in Table 1; (2) the main diffraction line at 2θ ca. 28.6° is progressively shifted toward higher diffraction angles and the lattice parameter of $Ce_xZr_{1-x}O_2$ mixed oxides decreases from 5.4112 to 5.3049 Å as the Ce content decreases from 1 to 0.5 at.%. This contraction of the oxide cell is due to the substitution of the cerium atoms (1.09 Å) by the smaller Zr atoms (0.86 Å). Moreover, this linear variation of the lattice parameter with the cerium content in the range 0.5–1 at.%, in agreement with the Vegard's law, confirms that these oxides exist as solid solutions. In addition, based on the Vegard's law and using some standard diffraction data from the ICDD database obtained on well-defined crystals (ICDD files nos. 43-1002, 28-0271, 38-1439 and 04-002-2714), the crystal composition of the mixed oxides could be extracted from those XRD results. The only major deviation compared to the "theoretical" mixed oxide composition was observed for the $Ce_{0.65}Zr_{0.35}O_2$ sample when the crystal appeared to be richer in cerium compared to the theoretical composition. Considering the elemental analysis determined by ICP-OES, which is conform to the theoretical composition, this observation would tend to indicate the presence of a separate zirconium-rich phase, which would be XRD-invisible, i.e. either an amorphous or a very well-dispersed phase.

At low Ce content (0.16 at.%), the diffraction pattern is characteristic of the tetragonal structure, the same as for pure ZrO_2.

The pH at the point of zero charge (pH_{PZC}) of the different $Ce_xZr_{1-x}O_2$ mixed oxides ranges from 7.4 to 5.4, somehow decreasing with increasing the Zr content, as already observed. The cerium-rich solid solutions, as prepared here, are essentially neutral while the zirconium-rich oxides would tend to be slightly acidic. In any case, all catalyst surfaces would globally be positively charged under the applied acidic reaction conditions.

Finally, the surface area of the $Ce_xZr_{1-x}O_2$ mixed oxides is higher than that of pure CeO_2 and ZrO_2, indicating that the addition of Zr is helpful to stabilize the oxide structure and prevent sintering. These results are in good agreement with the evolution of the oxide crystallite size derived from the XRD results (Table 1).

3.2. Catalytic wet air oxidation

First, the thermal stability of the formic acid molecule under the applied reaction conditions was evaluated. In the absence of any catalytic solid in the reactor, no detectable conversion was ever detected, even after 8 h of reaction at 326 K.

Then, as a preliminary work, the effect of the catalyst loading was evaluated. The objective was to exclude any diffusion limitation and insure the reaction to be performed under chemical control. Fig. 2 shows the effect of the 0.1 wt.%Pt/$Ce_{0.9}Zr_{0.1}O_2$ catalyst loading (0.2, 0.35, 0.5, 0.7 and 1.0 g L^{-1}) on the conversion of formic acid (5 g L^{-1}) at 326 K under atmospheric pressure. As expected, the overall conversion increased as the catalyst loading increased from 0.2 to 0.7 g L^{-1}. As a result, the initial reaction rate, expressed per gram of active phase, remained constant at ca. 84–92 $mol_{FA}\,h^{-1}\,g_{Pt}{}^{-1}$ (89 $mol_{FA}\,h^{-1}\,g_{Pt}{}^{-1}$ on average). At higher catalyst loading, the conversion did not significantly change anymore and the initial reaction rate decreased to 66 $mol_{FA}\,h^{-1}\,g_{Pt}{}^{-1}$ at 1.0 g L^{-1}. In conclusion, the reaction might be assumed to be operated under kinetic control whenever the catalyst loading is lower or equal to 0.7 g L^{-1}. In the following, all experiments were carried out using a 0.5 g L^{-1} catalyst loading.

3.2.1. Effect of the support composition

A series of experiments using the different $Ce_xZr_{1-x}O_2$-supported Pt catalysts were performed in the CWAO of formic acid at 326 K under atmospheric pressure (air flow: 0.45 L min^{-1}). The objective was a better understanding of the $Ce_xZr_{1-x}O_2$ support composition effect on the catalytic performances. Indeed, it was earlier shown that the ruthenium catalyst performances in the CWAO of acetic acid (473 K, 3.8 MPa total pressure) strongly depend on the nature of the support (CeO_2, TiO_2 and ZrO_2) [40].

The bare $Ce_xZr_{1-x}O_2$ mixed oxides demonstrated low activities. Only ca. 10% formic acid conversion was achieved after 6 h reaction (not shown).

Fig. 3 shows the evolution of the formic acid conversion as a function of reaction time in the CWAO of formic acid over a series of 0.5 wt.%Pt/$Ce_xZr_{1-x}O_2$ catalysts (theoretical Pt loading). The Pt catalysts exhibited high activities; even at 326 K. 100% formic acid conversion was obtained after maximum 120 min reaction, except in the case of the 0.400 wt.%Pt/CeO_2 and 0.335 wt.%Pt/$Ce_{0.16}Zr_{0.84}O_2$ catalysts (30% and 87% conversion after 120 min reaction, respectively). High initial reaction rates, expressed in mole of formic acid converted per hour and per gram of platinum in the sample, were calculated (Table 2). Indeed, the 0.385 wt.%Pt/$Ce_{0.9}Zr_{0.1}O_2$ catalyst showed a higher activity, expressed per gram of Pt, compared to the 1.5 wt.%Pt/C and 0.7 wt.%Pt/Al_2O_3 catalysts, as earlier reported in the literature [27,29]. Furthermore, it is observed that the support composition

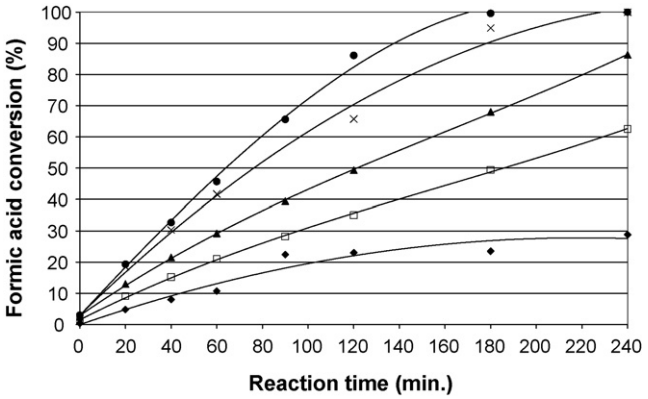

Fig. 2. CWAO of formic acid (5 g L^{-1}) at 326 K under atmospheric pressure over 0.1 wt.%Pt/$Ce_{0.9}Zr_{0.1}O_2$. Impact of the catalyst loading (0.2 (♦), 0.35 (□), 0.5 (▲), 0.75 (×) and 1 (●) g L^{-1}).

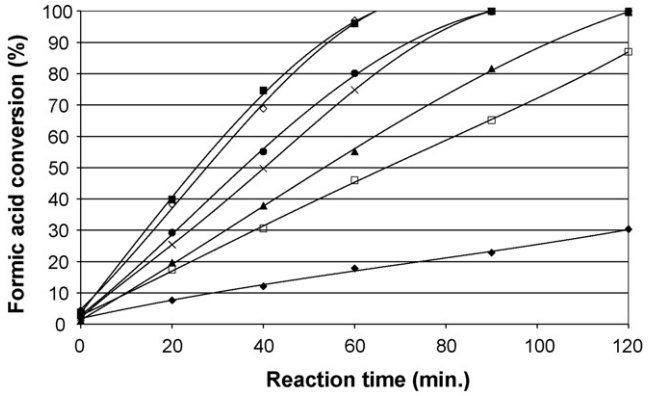

Fig. 3. CWAO of formic acid (5 g L^{-1}) at 326 K under atmospheric pressure over 0.5 wt.%Pt/$Ce_xZr_{1-x}O_2$ (0.5 g L^{-1} catalyst). Impact of the support composition (x = 0 (×), 0.16 (□), 0.5 (▲), 0.65 (●), 0.75 (◊), 0.9 (■) and 1 (♦)).

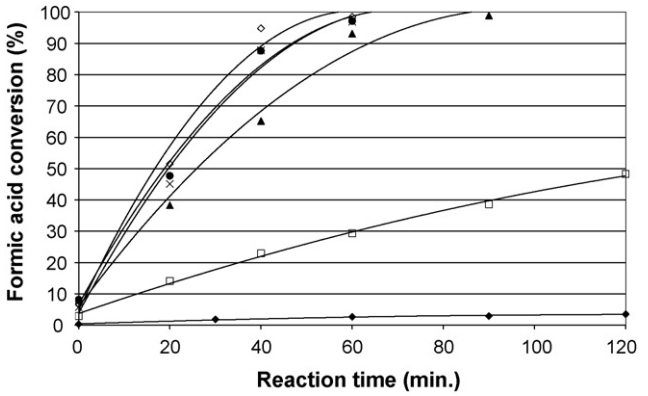

Fig. 4. CWAO of formic acid (5 g L^{-1}) over Pt/$Ce_{0.9}Zr_{0.1}O_2$ (0.5 g L^{-1} catalyst) at 326 K under atmospheric pressure. Impact of the Pt loading (0.014 (♦), 0.080 (□), 0.230 (▲), 0.300 (●), 0.385 (×) and 0.770 (◊) wt.%Pt).

obviously affected Pt catalyst performances. The activity gradually increased with increasing the Ce content in the $Ce_xZr_{1-x}O_2$ mixed oxides. The initial reaction rate increased from 30 to 67 $mol_{FA}\,h^{-1}\,g_{Pt}{}^{-1}$ with increasing the Ce content from 0.16 to 0.9. Furthermore, a very good correlation was observed between the initial reaction rate and the effective mixed oxide composition deduced from the XRD analysis, underlying the influence of the composition on the oxide structure and their reactivity towards oxygen. The 0.385 wt.%Pt/$Ce_{0.9}Zr_{0.1}O_2$ catalyst showed the best activity.

Upon CWAO using simple-oxide supported catalysts, it is well known that the oxygen transfer from the solution to the active sites on the catalyst surface is rate limiting. This step is expected to be accelerated on the $Ce_xZr_{1-x}O_2$ supports with a fluorite-type of structure. Indeed, the amount of oxygen vacancies at the $Ce_xZr_{1-x}O_2$ solid solutions surface is much higher compared to pure CeO_2 and ZrO_2. Such vacancies may induce the formation of highly reactive surface oxygen species such as peroxides ($O_2{}^-$) and/or superoxides ($O_2{}^{2-}$) [33–35]. As a result, the $Ce_xZr_{1-x}O_2$-supported Pt catalysts showed higher activities in the CWAO of formic acid compared to the Pt/CeO_2 or Pt/ZrO_2 catalysts.

3.2.2. Effect of the Pt loading

Six different $Ce_{0.9}Zr_{0.1}O_2$-supported Pt catalysts, containing 0.02, 0.1, 0.3, 0.4, 0.5 and 1 wt.%Pt (theoretical loading), were prepared. Indeed, the Pt dispersion on the support might vary as a function of the Pt loading and the catalytic performances might be consequently affected. Fig. 4 shows the evolution of the formic acid conversion upon CWAO at 326 K under atmospheric pressure. Formic acid conversion increased with increasing Pt loading. The conversion increased from 3%, 29%, 93%, 97%, 97% to 99% after 60 min reaction when the Pt loading changed from 0.014, 0.080, 0.230, 0.300, 0.385 to 0.770 wt.%, respectively. Moreover, in the range 0.230–0.770 wt.%, 100% formic acid conversion was achieved after 90 min reaction and the conversion did not change further with increasing the Pt loading. The same tendencies could be observed looking at the initial reaction rates expressed in mole of formic acid converted per gram of Pt and per hour (Table 3). As far as the reaction is operated under chemical control, a constant value would be expected, if the Pt dispersion would be constant, whatever the Pt loading. However, our results tend to indicate that the Pt particle size increases with increasing the Pt loading above 0.300 wt.%. The optimum platinum loading on the $Ce_{0.9}Zr_{0.1}O_2$ support, leading the best catalytic performances, was shown to be somehow between 0.080 and 0.300 wt.%.

The chemical stability of the 0.080 and 0.385 wt.%Pt/$Ce_{0.9}Zr_{0.1}O_2$ catalysts, with the best activity, was investigated. After 240 min reaction, neither platinum, nor cerium, nor zirconium could be detected via ICP-OES ($\leq$0.1 mg L^{-1}). These results indicate that the Pt/$Ce_{0.9}Zr_{0.1}O_2$ catalysts are stable towards leaching in the CWAO of formic acid at 326 K under atmospheric pressure.

3.2.3. Effect of the reaction temperature

The reaction temperature is an important parameter affecting the CWAO initial reaction rate. A series of experiments were performed at ca. 294, 304, 313, and 326 K under atmospheric pressure. The results obtained over 0.080 wt.%Pt/$Ce_{0.9}Zr_{0.1}O_2$ are shown in Fig. 5. Conversions in formic acid ranged from 39% to 100% after 6 h depending on the reaction temperature. In the meantime, the initial reaction rate varied from 21, 43, 64 to 89 $mol_{FA}\,h^{-1}\,g_{Pt}{}^{-1}$ as the temperature increased from 294 to 326 K (Table 4). From the Arrhenius plot, the activation energy of the formic acid CWAO over the 0.080 wt.%Pt/$Ce_{0.9}Zr_{0.1}O_2$ catalyst was calculated to be ca. 36 ± 4 kJ mol^{-1}. This value is completely comparable to what has been earlier reported in the literature by Gallezot et al. [27] in the case of 1.56 wt.%Pt/C (26.4 kJ mol^{-1}) and by Gunduz et al. in the case of 0.7 wt.%Pt/Al_2O_3

Table 2
Formic acid CWAO over 0.5 wt.%Pt/$Ce_xZr_{1-x}O_2$ catalysts (theoretical Pt loading) at 326 K under atmospheric pressure [5 g L^{-1} formic acid, 0.5 g L^{-1} catalyst] – influence of the mixed oxide support composition.

Samples	Initial reaction rate ($mol_{FA}\,h^{-1}\,g_{Pt}{}^{-1}$)
0.400 wt.%Pt/CeO_2	9
0.385 wt.%Pt/$Ce_{0.9}Zr_{0.1}O_2$	67
0.395 wt.%Pt/$Ce_{0.75}Zr_{0.25}O_2$	57
0.285 wt.%Pt/$Ce_{0.65}Zr_{0.35}O_2$	64
0.285 wt.%Pt/$Ce_{0.5}Zr_{0.5}O_2$	45
0.335 wt.%Pt/$Ce_{0.16}Zr_{0.84}O_2$	30
0.365 wt.%Pt/ZrO_2	46

Table 3
Formic acid CWAO over $Ce_{0.9}Zr_{0.1}O_2$-supported platinum catalysts at 326 K under atmospheric pressure [5 g L^{-1} formic acid, 0.5 g L^{-1} catalyst] – influence of the Pt loading.

Samples	Initial reaction rate ($mol_{FA}\,h^{-1}\,g_{Pt}{}^{-1}$)
0.014 wt.%Pt/$Ce_{0.9}Zr_{0.1}O_2$	56
0.080 wt.%Pt/$Ce_{0.9}Zr_{0.1}O_2$	89
0.230 wt.%Pt/$Ce_{0.9}Zr_{0.1}O_2$	89
0.300 wt.%Pt/$Ce_{0.9}Zr_{0.1}O_2$	95
0.385 wt.%Pt/$Ce_{0.9}Zr_{0.1}O_2$	67
0.770 wt.%Pt/$Ce_{0.9}Zr_{0.1}O_2$	41

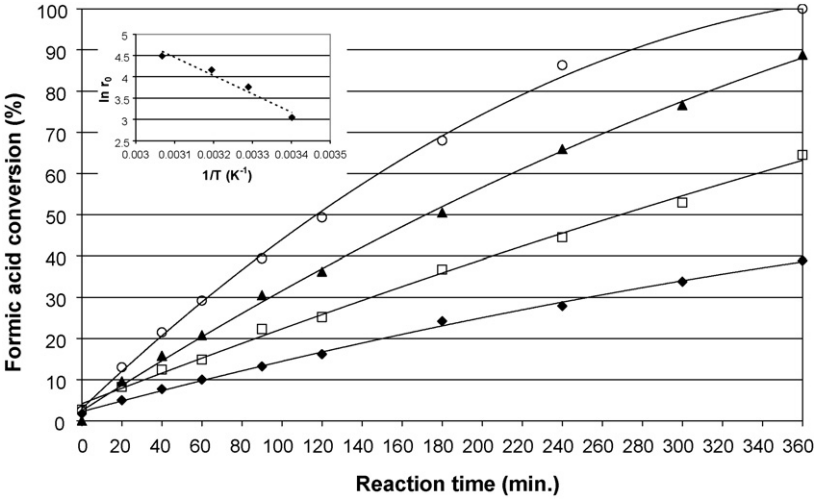

Fig. 5. CWAO of formic acid (5 g L^{-1}) over 0.080 wt.%Pt/$Ce_{0.9}Zr_{0.1}O_2$ (0.5 g L^{-1}) under atmospheric pressure. Impact of the reaction temperature (294 (♦), 304 (□), 313 (▲) and 326 (○) K) [The insert in the upper left corner is the Arrhenius plot].

Table 4
Formic acid CWAO over 0.080 wt.%Pt/$Ce_{0.9}Zr_{0.1}O_2$ catalyst under atmospheric pressure [5 g L^{-1} formic acid, 0.5 g L^{-1} catalyst] – influence of the reaction temperature.

Temperature (K)	Initial reaction rate (mol_{FA} h^{-1} $g_{Pt}{}^{-1}$)
326	89
313	64
304	43
294	21

(24.6 kJ mol^{-1}) [29]. Furthermore, in the absence of any catalyst, the activation energy for the WAO of formic acid was ca. 149 kJ mol^{-1}. In conclusion, the 0.080 wt.%Pt/$Ce_{0.9}Zr_{0.1}O_2$ catalyst may efficiently decrease the reaction activation energy and, consequently, significantly accelerates the oxidation of formic acid.

3.2.4. Effect of the initial concentration in formic acid

The effect of the initial formic acid concentration on the activity of 0.080 wt.%Pt/$Ce_{0.9}Zr_{0.1}O_2$ was investigated at different temperatures, namely ca. 294, 313 and 326 K. As an example, Fig. 6 shows the evolution of the formic acid conversion at 326 K under atmospheric pressure for different initial concentrations in formic acid: 500, 1000, 2500 and 5000 mg L^{-1}. The lower the initial concentration, the faster 100% conversion was achieved: 90, 240, 240 and 360 min, respectively.

At 326 K, the initial reaction rate increased from 15 to 89 mol_{FA} h^{-1} $g_{Pt}{}^{-1}$ as the initial concentration of formic acid increased from ca. 250 to 5000 mg L^{-1}. This trend indicates a positive reaction order with respect to the formic acid concentration. Indeed, the reaction order with respect to formic acid is about 0.5 ± 0.1 at 326 K.

On the opposite, at 313 K, the initial formic acid conversion rate appeared to be about constant at ca. 70 mol_{FA} h^{-1} $g_{Pt}{}^{-1}$ (Table 5). The same type of results was observed at 294 K when the concentration in formic acid increased from 1000 to 5000 mg L^{-1}. In conclusion, the initial concentration in formic acid does not have much effect anymore on the initial reaction rate in the lower reaction temperature range ($T \leq 313$ K). Then, the reaction order with respect to formic acid is about zero in the CWAO of formic acid over 0.080 wt.%Pt/$Ce_{0.9}Zr_{0.1}O_2$ below 313 K.

The differences observed, depending on the reaction temperature, are a clear evidence of different kinetic regimes. In the CWAO of organic compounds, it is classically reported in the literature that the competitive adsorption between the oxygen and the organic compound to be oxidized tends to control the initial reaction rate. Indeed, in the case of oxidations performed over catalysts

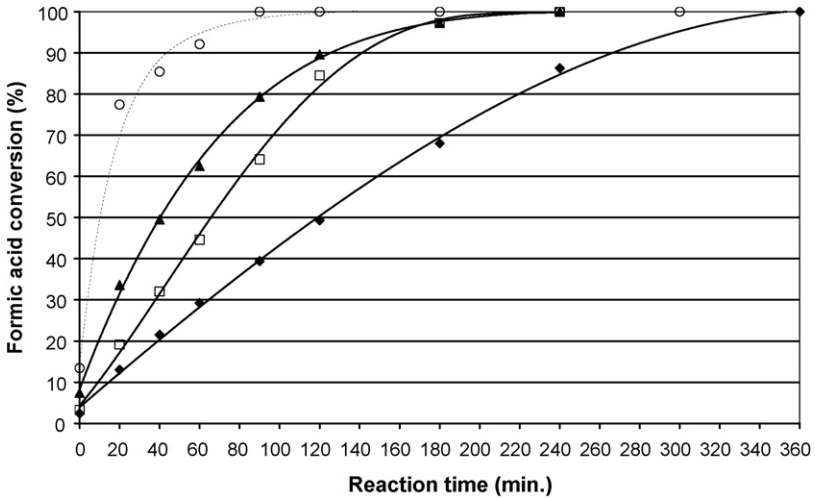

Fig. 6. CWAO of formic acid (5 g L^{-1}) over 0.080 wt.%Pt/$Ce_{0.9}Zr_{0.1}O_2$ (0.5 g L^{-1} catalyst) at 326 K under atmospheric pressure. Impact of the initial formic acid concentration (500 (○), 1000 (▲), 2500 (□) and 5000 (♦) mg L^{-1}).

Table 5
Formic acid CWAO over 0.080 wt.%Pt/$Ce_{0.9}Zr_{0.1}O_2$ catalyst under atmospheric pressure [0.5 g L^{-1} catalyst] – influence of the initial formic acid concentration as a function of the reaction temperature.

Temperature (K)	Formic acid concentration (mg L^{-1})	Initial reaction rate (mol_{FA} h^{-1} $g_{Pt}{}^{-1}$)
326	250	15
	500	32
	1000	46
	5000	89
313	1000	73
	2500	68
	5000	64
294	500	21
	1000	20
	2500	27
	5000	21

supported on conventional supports, such as TiO_2, ZrO_2, etc., the hydrocarbon is strongly adsorbed on the catalyst surface and the oxygen activation/adsorption at the active site is the rate determining step. In our case, at low temperature ($T \leq 313$ K), formic acid is strongly adsorbed and saturates the surface, so that oxygen may hardly adsorb. In such a situation, the initial reaction rate (i) is independent on the concentration in formic acid, but (ii) should directly depend on the dissolved O_2 concentration. As a result, the reaction order with respect to formic acid is zero, as observed in this study at low temperature ($T \leq 313$ K). At higher temperature (326 K), the adsorption strength of formic acid on the catalyst surface is somehow weakened and the formic acid surface coverage goes below unity. The oxygen adsorption is consequently more favorable; especially with the "help" of the mixed oxide supports once the energetic barrier for oxygen diffusion in these solids is overcame. In that case, the initial reaction rate depends on both the formic acid and oxygen concentrations and the reaction orders get higher than 0 (0.5 ± 0.1 in our study) and lower than 1 with respect to formic acid and oxygen, respectively.

3.2.5. *Effect of the dissolved oxygen concentration*

In order to quantify the influence of the oxygen partial pressure, the CWAO of formic acid (5 g L^{-1}) over the 0.080 wt.%Pt/$Ce_{0.9}Zr_{0.1}O_2$ catalyst was studied under either air (20% O_2 in N_2) or pure oxygen.

In the 294–326 K temperature range, the formic acid conversion markedly increased with the substitution of air for oxygen. For example, at RT, the conversion of formic acid increased from 40% to 90% after 360 min reaction going from synthetic air to pure O_2. In the same way, at 313 K, when pure oxygen was used, 100% formic acid conversion was achieved after 90 min reaction, while only 90% formic acid removal was obtained under synthetic air after 360 min of reaction.

Table 6
Formic acid CWAO over 0.080 wt.%Pt/$Ce_{0.9}Zr_{0.1}O_2$ catalyst under atmospheric pressure [5 g L^{-1} formic acid] – influence of the initial oxygen partial pressure as a function of the reaction temperature.

Reaction temperature (K)	Oxidant	Initial reaction rate (mol_{FA} h^{-1} $g_{Pt}{}^{-1}$)
326	O_2	341
	Air	89
313	O_2	296
	Air	64
294	O_2	96
	Air	21

At 294 and 313 K, as summarized in Table 6, the initial reaction rate increased from 21 and 64 to 96 and 296 mol_{FA} h^{-1} $g_{Pt}{}^{-1}$ going from air to pure oxygen, respectively. In both cases, the reaction order with respect to oxygen was calculated to be ca. 1 ± 0.1. This result indicated that the oxygen activation/transfer up to the active site was somehow limiting up to 313 K, potentially due to the strong adsorption of formic acid (see Section 3.2.4).

In turn, at 326 K, the initial reaction rate only increased from 89 to 341 mol_{FA} h^{-1} $g_{Pt}{}^{-1}$ with the substitution of air for oxygen, corresponding to a reaction order with respect to oxygen ca. 0.8 ± 0.1. This result indicated that, at higher reaction temperature, the effect of the oxygen activation/transfer to the active site on the reaction rate is less pronounced. This observation might be directly put in parallel with the decrease of the adsorption strength of formic acid on the catalyst surface, as demonstrated in the previous paragraph. Moreover, we could check the reaction mechanism was not significantly modified upon reaction under pure oxygen since the reaction apparent activation energy was ca. 33 ± 4 kJ mol^{-1}, vs. 36 ± 4 kJ mol^{-1} under synthetic air. These results confirmed the potential implication of the mixed oxide supports in the oxygen activation/transfer processes whenever the oxygen diffusion barriers in these materials are overcame, i.e. at temperatures higher than 326 K in the present case.

4. Conclusions

A large variety of Pt/$Ce_xZr_{1-x}O_2$ catalysts were investigated in the CWAO of formic acid under moderate reaction conditions (294–326 K, atmospheric pressure). The 0.080 wt.%Pt/$Ce_{0.9}Zr_{0.1}O_2$ catalyst showed the highest activity. Moreover, it was demonstrated to be chemically stable. The reaction activation energy was ca. 36 ± 4 kJ mol^{-1}. Up to 313 K, the initial reaction rate classically depended on the only dissolved oxygen concentration in the solution. The reaction order with respect to formic acid was 0 ± 0.1, while the reaction order with respect to oxygen was ca. 1 ± 0.1. However, at 326 K, both the formic acid and oxygen concentrations influenced the initial reaction rate. The reaction order with respect to formic acid was increased to ca. 0.5 ± 0.1 while the reaction order with respect to oxygen decreased to ca. 0.8 ± 0.1. These changes in the reaction kinetics, from ca. 326 K, clearly evidenced the possible role of the ceria–zirconia mixed oxide supports in the oxygen activation processes, whenever the oxygen activation barrier directly onto the support is overcame.

Acknowledgments

The authors are sincerely grateful to the French Ministry of Foreign Affairs and the Région Rhône-Alpes for financial supports under programs ARCUS Chine, MIRA 2006 and MIRA 2007, including Ms. Shaoxia Yang post-doctoral fellowship from April 2007 to January 2009.

References

[1] X. Zhu, S. Shi, J. Wei, F. Lv, H. Zhao, J. Kong, Q. He, J. Ni, Environ. Sci. Technol. 41 (2007) 6541.
[2] W.Y. Han, P.Y. Zhang, W.P. Zhu, J.J. Yin, L.S. Li, Water Res. 38 (2004) 4197.
[3] V.S. Mishra, V.V. Mahajani, J.B. Joshi, Ind. Eng. Chem. Res. 34 (1995) 2.
[4] F. Luck, Catal. Today 53 (1999) 81.
[5] J. Levec, A. Pintar, Catal. Today 24 (1995) 51.
[6] F. Luck, Catal. Today 27 (1996) 195.
[7] J.E. Atwater, J.R.A. Akse, J.A. McKinnis, J.O. Thompson, Chemosphere 34 (1997) 203.
[8] Y.I. Matatov-Meytal, M. Sheintuch, Ind. Eng. Chem. Res. 37 (1998) 309.
[9] S. Imamura, Ind. Eng. Chem. Res. 38 (1999) 1743.
[10] A. Pintar, M. Besson, P. Gallezot, J. Gibert, D. Martin, Water Res. 38 (2004) 289.
[11] D.P. Minh, P. Gallezot, M. Besson, Appl. Catal. B: Environ. 63 (2006) 68.
[12] N. Li, C. Descorme, M. Besson, Appl. Catal. B: Environ. 71 (2007) 262.

[13] G. Ovejero, J.L. Sotelo, A. Rodriguez, C. Diaz, R. Sanz, J. Garcia, Ind. Eng. Chem. Res. 46 (2007) 6449.
[14] J. Mikulova, S. Rossignol, J. Barbier Jr., D. Mesnard, C. Kappenstein, D. Duprez, Appl. Catal. B: Environ. 72 (2007) 1.
[15] J.B. Wang, W.P. Zhu, S.X. Yang, W. Wang, Y.R. Zhou, Appl. Catal. B: Environ. 78 (2008) 30.
[16] M.E. Suarez-Ojeda, F. Stüber, A. Fortuny, A. Fabregat, J. Carrera, J. Font, Appl. Catal. B: Environ. 58 (2005) 105.
[17] M.E. Suarez-Ojeda, A. Fabregat, F. Stüber, A. Fortuny, J. Carrera, J. Font, Chem. Eng. J. 132 (2007) 105.
[18] S.X. Yang, W.P. Zhu, X. Li, J.B. Wang, Y.R. Zhou, Catal. Commun. 8 (2007) 2059.
[19] S.X. Yang, X. Li, W.P. Zhu, J.B. Wang, C. Descorme, Carbon 46 (2008) 445.
[20] J. Guo, M. Al-Dahhan, Appl. Catal. A: Gen. 299 (2006) 175.
[21] Y. Liu, D.Z. Sun, Appl. Catal. B: Environ. 72 (2007) 205.
[22] M.H. Kim, K.H. Choo, Catal. Commun. 8 (2007) 462.
[23] S.S. Lin, C.L. Chen, D.J. Chang, C.C. Chen, Water Res. 36 (2002) 3009.
[24] S.X. Yang, W.P. Zhu, J.B. Wang, J.B. Wang, Z.X. Chen, J. Hazard. Mater. 153 (2008) 1248.
[25] R.V. Shende, V.V. Mahajani, Ind. Eng. Chem. Res. 36 (1997) 4809.
[26] R.V. Shende, J. Levec, Ind. Eng. Chem. Res. 38 (1999) 3830.
[27] P. Gallezot, S. Chaumet, A. Perrard, P. Isnard, Appl. Catal. B: Environ. 9 (1996) L11.
[28] P. Gallezot, N. Laurain, P. Isnard, J. Catal. 168 (1997) 104.
[29] G. Gunduz, M. Dukkanci, Int. J. Chem. React. Eng. 5 (2007) 36.
[30] J. Mikulová, J. Barbier Jr., S. Rossignol, D. Mesnard, D. Duprez, C. Kappenstein, J. Catal. 251 (2007) 172.
[31] A. Pintar, J. Batista, T. Tisler, Appl. Catal. B: Environ. 84 (2008) 30.
[32] A. Trovarelli, C. de Leitenburg, M. Boaro, G. Dolcetti, Catal. Today 50 (1999) 353.
[33] A. Trovarelli (Ed.), Catalysis by Ceria and Related Materials, G.J. Hutchings (Series Ed.), Imperial College Press, London, 2002.
[34] N. Li, C. Descorme, M. Besson, Appl. Catal. B: Environ. 76 (2007) 92.
[35] N. Li, C. Descorme, M. Besson, Catal. Commun. 8 (2007) 1815.
[36] N. Li, C. Descorme, M. Besson, Appl. Catal. B: Environ. 80 (2008) 237.
[37] M.K. Oudenhuijzen, P.J. Kooyman, B. Tappel, J.A. van Bokhoven, D.C. Koningsberger, J. Catal. 205 (2002) 135.
[38] L. Vegard, Z. Phys. 5 (1921) 17.
[39] H. Moriwaki, Y. Yoshikawa, T. Morimoto, Langmuir 6 (1990) 847.
[40] J. Barbier Jr., F. Delanöe, F. Jabouille, D. Duprez, G. Blanchard, P. Isnard, J. Catal. 177 (1998) 378.